

Tuning a Resonance in the Fock Space: Optimization of Phonon Emission in a Resonant Tunneling Device

L. E. F. Foa Torres^a, H. M. Pastawski^{a*} and S. S. Makler^{b,c}

^aFacultad de Matemática, Astronomía y Física, Universidad Nacional de Córdoba, Ciudad Universitaria, 5000 Córdoba, Argentina.

^bInstituto de Física, Universidade do Estado do Rio de Janeiro, Caixa Postal 68.528, 21945-970 Rio de Janeiro, Brazil.

^cInstituto de Física, Universidade Federal Fluminense, Campus da Praia Vermelha, 24210-340 Niterói, Brazil.

(December 2, 2024)

Phonon-assisted tunneling in a double barrier resonant tunneling device can be seen as a resonance in the electron-phonon Fock space which is tuned by the applied voltage. We show that the geometrical parameters can induce a symmetry condition in this space that can strongly enhance the emission of longitudinal optical phonons. For devices with thin emitter barriers this is achieved by a wider collector barrier.

Progress in mesoscopic semiconductor devices [1] and molecular electronics [2] is driven by the need of miniaturization and the wealth of new physics provided by coherent quantum phenomena. A fundamental idea behind these advances was Landauer's view that *conductance is transmittance* [3,4]. Hence, the typical conductance peaks and valleys, observed when some control parameter is changed, are seen as fringes in an interferometer. However, the many-body electron-electron (e-e) and electron-phonon (e-ph) interactions restrict the use of this picture. While e-e effects received much attention in different contexts [1], interest on e-ph interaction remained focused on double barrier Resonant Tunneling Devices (RTD) [5], where phonon-assisted tunneling shows up as a satellite peak in a valley of the current-voltage (I-V) curve. Only recently, molecular electronics manifested [6] this phenomenon. Theory evolved from a many-body Green's function in a simplified model for the polaronic states [7] to quantum and classical rate equations approach [8]. The latter uses an incoherent description of the e-ph interaction by adopting an imaginary self-energy correction to the electronic states [9,10].

In this Letter, we analyze a quantum coherent solution of the e-ph interaction by mapping the many-body problem into a one-body scattering system where each phonon mode adds a new dimension to the electronic variable [11,12]. Transmission of electrons between incoming and outgoing channels with different number of phonons are then used in a Landauer's picture where the only incoherent processes occur inside the electrodes. This allows to develop the concept of *resonance in the e-ph Fock space* and the identification of the control parameters that optimize the coherent processes leading to a maximized phonon emission. It also gives a clue as to how "decoherence" arise within an exact many-body description. As an application, we consider a RTD phonon emitter in which the first polaronic excitation serves as an "intermediate" state for the phonon emission. An

electron with kinetic energy $\varepsilon \leq \varepsilon_F$ and potential energy eV in the emitter *decays through tunneling into* an electron with energy $\varepsilon + eV - \hbar\omega_0$ in the collector *plus* a longitudinal optical (LO) phonon. The tuning parameter is the applied voltage while the optimization of phonon emission requires the tailoring of the tunneling rates.

Let us consider a minimal Hamiltonian:

$$\mathcal{H} = \sum_j \{E_j c_j^+ c_j - V_{j,j+1}(c_j^+ c_{j+1} + c_{j+1}^+ c_j)\} + \hbar\omega_0 b^+ b - V_g c_0^+ c_0(b^+ + b), \quad (1)$$

where c_j^+ and c_j are electron creation and annihilation operators at site j on a 1-d chain with lattice constant a and hopping parameters $V_{j,j+1} = V$. Tunneling rates are fixed by $V_{0,1} = V_R$ and $V_{-1,0} = V_L$ ($V_{L(R)} \ll V$). The site energies are $E_j = 2V$ for $j < 0$ and $2V - eV$ for $j > 0$. $E_0 = E_{(o)} - \alpha eV$ is the well's *ground state* shifted by the electric field. For barrier widths L_L and L_R and well size L_W a linear approximation for the potential profile gives $\alpha = (L_L + L_W/2)/(L_L + L_W + L_R)$. We consider a single LO-phonon mode and an interaction (V_g) limited to the well. b^+ and b are the creation and annihilation operators for phonons. We restrict the Fock space to that expanded by $|j, n\rangle = c_j^+ (b^+)^n / \sqrt{n!} |0\rangle$, which maps to the 2-dimensional one-body problem shown in Fig. 1. The number n of phonons is the vertical dimension [11,12]. The horizontal dangling chains can be eliminated through a decimation procedure [10,13] leading to an effective Hamiltonian:

$$\tilde{\mathcal{H}}_{e-ph} = \sum_{n \geq 0} \{[E_0 + n\hbar\omega_0 + \Sigma_n(\varepsilon)] |0, n\rangle \langle 0, n| - \sqrt{n+1} V_g (|0, n+1\rangle \langle 0, n| + |0, n\rangle \langle 0, n+1|)\}, \quad (2)$$

The electron hopping into the electrodes is taken into account by the ε -dependence of the retarded self-energy corrections $\Sigma_n = {}^L\Sigma_n + {}^R\Sigma_n$. Specifically, ${}^L\Sigma_n = |V_L|^2 \times \Sigma(\varepsilon - n\hbar\omega_0)$, ${}^R\Sigma_n = |V_R|^2 \times \Sigma(\varepsilon - n\hbar\omega_0 + eV)$, with:

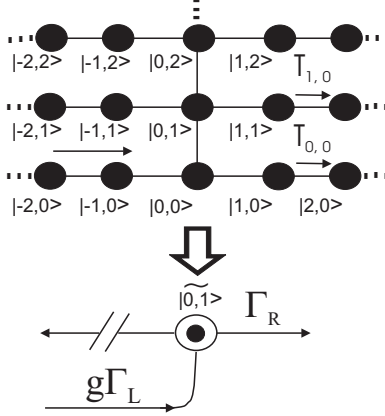


FIG. 1. Simple model: dots are states in the Fock space, lines are interactions. The effective Hamiltonian for the first polaronic excitation is represented at the bottom.

$$\Sigma(\varepsilon) = \Delta(\varepsilon) - i\Gamma(\varepsilon); \quad \Delta(\varepsilon) = \frac{1}{\pi} \int \frac{\Gamma(\varepsilon')}{\varepsilon - \varepsilon'} d\varepsilon',$$

$$\Gamma(\varepsilon) = \sqrt{V^2 - (\varepsilon/2 + V)^2} \times \theta(\varepsilon) \times \theta(4V - \varepsilon). \quad (3)$$

While the imaginary part $\Gamma = \hbar v_\varepsilon/a$ is proportional to the group velocity v_ε in the electrodes, the actual escape rates $\Gamma_{L(R)}/\hbar$ are barrier controlled. For width $L_{L(R)}$ and attenuation length ξ , $\Gamma_{L(R)}/\Gamma = |V_{L(R)}/V|^2 \simeq \exp[-L_{L(R)}/\xi]$.

The retarded Green function connecting states i and n ,

$$G_{n,i}^R(\varepsilon) = \langle 0, n | (\varepsilon \mathcal{I} - \tilde{\mathcal{H}}_{e-ph}(\varepsilon))^{-1} | 0, i \rangle, \quad (4)$$

has poles at the exact eigenenergies. If $\Sigma_n(\varepsilon) \equiv 0$, these are the polaronic energies $E_0 - \frac{|V_g|^2}{\hbar\omega_0} + n\hbar\omega_0$. The transmission coefficient $T_{n,i}$ from the i -th incoming channel at left electrode to the n -th channel at right is [10]:

$$T_{n,i}(\varepsilon) = 2 \operatorname{Im}^R \Sigma_n(\varepsilon) |G_{n,i}^R(\varepsilon)|^2 2 \operatorname{Im}^L \Sigma_i(\varepsilon). \quad (5)$$

If the Fermi energy $\varepsilon_F \ll V$, Eq.(3) becomes:

$$\Sigma(\varepsilon) \approx -i\Gamma(\varepsilon = \varepsilon_F) \times \theta(\varepsilon), \quad (6)$$

and the θ -function may cancel some T 's.

To obtain the *elastic transmittance* when $g = (V_g/\hbar\omega_0)^2 \ll 1$ and $(\varepsilon_F, \Gamma_L + \Gamma_R) < \hbar\omega_0$, we need:

$$G_{0,0}^R \simeq \frac{1-g}{\varepsilon - \bar{E}_0 + i[\Gamma_L + \Gamma_R]} +$$

$$+ \frac{g}{\varepsilon - [\bar{E}_0 + \hbar\omega_0] + i[\tilde{\Gamma}_L + \Gamma_R]}, \quad (7)$$

evaluated with the first two polaronic states. Here, $\tilde{\Gamma}_L = g\Gamma_L$ and $\bar{E}_0 = E_0 - \frac{|V_g|^2}{\hbar\omega_0}$. The first term contains the main resonance associated to the build up of

the polaronic ground state. The second term contains a virtual exploration into the first polaronic excitation. It is noteworthy that when $\Gamma = 0$, this Green function would cancel out at an intermediate energy giving rise to an *antiresonance* [14,13]. This concept extends the spectroscopic Fano-resonances [15] to the problem of conductance [16]. For $g \ll 1$, this effect is less important and in the whole energy range,

$$T_{0,0} \simeq \frac{4\Gamma_L\Gamma_R}{[\varepsilon - \bar{E}_0]^2 + [\Gamma_L + \Gamma_R]^2} + \mathcal{O}(g) \quad (8)$$

describes the main resonant elastic peak at $\varepsilon = \bar{E}_0$.

The *inelastic transmittance*, $T_{1,0}$, can be evaluated from:

$$G_{1,0}^R \simeq \frac{-\frac{V_g}{\hbar\omega_0}}{\varepsilon - \bar{E}_0 + i[\Gamma_L + \Gamma_R]} +$$

$$+ \frac{\frac{V_g}{\hbar\omega_0}}{\varepsilon - [\bar{E}_0 + \hbar\omega_0] + i[\tilde{\Gamma}_L + \Gamma_R]}. \quad (9)$$

When $\varepsilon + eV > \hbar\omega_0$ escapes are enabled and its poles involve the processes represented in the inset of Fig. 2: a) The first term gives an inelastic transmittance at the main peak. b) The second term provides a satellite peak at $\varepsilon = \bar{E}_0 + \hbar\omega_0$, associated to a polaronic excitation followed by its decay into an escaping electron and a phonon left behind. Around this satellite peak:

$$T_{1,0} \simeq \frac{4\tilde{\Gamma}_L\Gamma_R}{[\varepsilon - (\bar{E}_0 + \hbar\omega_0)]^2 + [\tilde{\Gamma}_L + \Gamma_R]^2}, \quad (10)$$

showing that phonon emission is a *resonance in the Fock-space* (see bottom of Fig. 1). A maximal probability ($T_{1,0} = 1$) requires equal rates of formation and decay [14]: $\tilde{\Gamma}_L = \Gamma_R$, which in our RTD implies:

$$\Gamma_R \simeq L_L + 2\xi \ln\left[\frac{\hbar\omega_0}{V_g}\right]. \quad (11)$$

Hence, thin barriers with this generalized symmetry condition have $T_{1,0} \simeq 1$ over a broad energy range.

The application of the Keldysh formalism [17] to our Fock-space gives an electrical current I_{tot} expressed as a balance equation [4] in terms of the transmittances of Eq. (5) and the electrochemical potentials. The experimental condition of high bias and low temperature ($eV > \varepsilon_F \gg k_B T$), rules out right-to-left flow, while $\hbar\omega_0 > \varepsilon_F$, enables the θ in Eq. (6) preventing inelastic reflection and overflow [18] of the final states. Thus,

$$I_{\text{tot}} = \sum_n I_n; \quad \text{where } I_n = \left(\frac{2e}{h}\right) \int_0^{\varepsilon_F} T_{n,0}(\varepsilon) d\varepsilon, \quad (12)$$

The “decoherence” introduced by the e-ph interaction on

the former single particle description can be now appreciated. One aspect, valid even if $\hbar\omega_0 \rightarrow 0$, is that in Eq. (12) the outgoing currents can not interfere. Another is the phase-shift fluctuations and “broadening” of the one-particle resonant energy induced by the virtual processes in the elastic channel of Eq. (7).

At the satellite peak, the main elastic contribution to the current is provided by the off-resonant tunneling through the ground state, i.e. $I_0 \simeq \frac{2e}{\hbar} 4\Gamma_L \Gamma_R \varepsilon_F / (\hbar\omega_0)^2$. The inelastic current determined by Eqs.(10) and (12) is

$$I_1 \simeq \frac{e}{\hbar} \frac{4\tilde{\Gamma}_L \Gamma_R}{(\tilde{\Gamma}_L + \Gamma_R)} \times \left[\frac{2}{\pi} \arctan \left(\frac{\varepsilon_F}{2(\tilde{\Gamma}_L + \Gamma_R)} \right) \right] \quad (13)$$

$$\simeq \begin{cases} \frac{e}{\hbar} 4\tilde{\Gamma}_L \Gamma_R / (\tilde{\Gamma}_L + \Gamma_R) & \text{for } \varepsilon_F \gg (\tilde{\Gamma}_L + \Gamma_R) \\ \frac{2e}{\hbar} T_{1,0}(\bar{E}_0 + \hbar\omega_0) \times \varepsilon_F & \text{for } \varepsilon_F \ll (\tilde{\Gamma}_L + \Gamma_R) \end{cases} .$$

The first line differs from the result of rate equations in [8] by the factor in brackets, fundamental to resolve extreme regimes. When $\varepsilon_F \gg (\tilde{\Gamma}_L + \Gamma_R)$ the inelastic current becomes geometry independent in the wide range of $\varepsilon_F \gg \Gamma_R > \tilde{\Gamma}_L$. In the opposite case I_1 , and hence the power emitted as phonons $\hbar\omega_0 I_1 / e$, becomes determined by the transmittance at resonance, which is maximized by the generalized symmetry condition of Eq. (11).

Each current term, $I_{n>0}$, contributes with n useful phonons, while I_0 ’s energy degrades fully into electrode heating. Then, one might seek a maximal ratio between the inelastic power P_{in} and the total power P ,

$$\eta = \frac{P_{\text{in}}}{P} = \frac{\hbar\omega_0 \sum_{n>0} n \frac{I_n}{e}}{I_{\text{tot}} V}, \quad (14)$$

which is the efficiency to transform the electric potential energy into LO-phonon energy. At the voltage tuning the resonance at the satellite peak $V_0 \simeq (E_{(o)} - |V_g|^2 / \hbar\omega_0 + \hbar\omega_0 - \varepsilon_F/2) / \alpha$, the lowest order of η has two factors $I_1 / (I_0 + I_1)$ and $\hbar\omega_0 / eV_0$. The first is small for narrow barriers because non-resonant tunneling dominates over phonon-assisted tunneling. For wide barriers, it goes to one as $\tilde{\Gamma}_L + \Gamma_R \rightarrow 0$. The second decreases with increasing right barrier’s width because it requires a higher V_0 . Thus, as Γ_R is decreased, two effects compete: the switch from non-resonant to phonon assisted resonant tunneling and an excess in the electronic kinetic energy in the collector. Hence, as long as the left barrier is not extremely thin ($\Gamma_L > \hbar\omega_0$), η can not depend much on geometry. With this restriction in mind, a device designed for phonon production should maximize the emitted power according to Eq. (11).

Let us compare these basic predictions with the numerical results of a description involving geometry, voltage and energy dependences of a typical RTD. A discrete 3-d model is defined in terms of the effective mass m^* with $V = \hbar^2 / (2m^* a^2)$. The potential profile for the diagonal energies E_j is shown in the inset of Fig. 2. N_L , N_R and

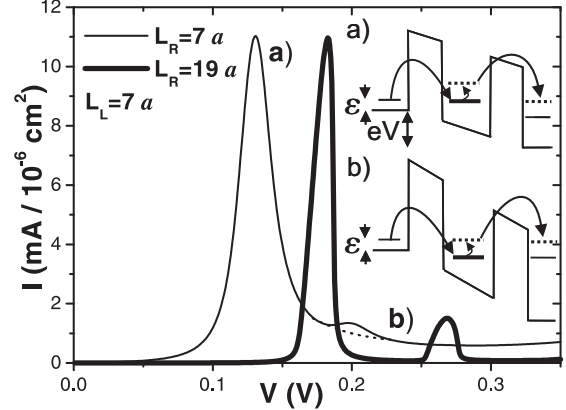


FIG. 2. Current density as a function of the applied voltage for a symmetrical (thin line) and optimized (thick line) structures with $L_L = 7a$ (19.7 Å). The dotted line indicates the background current in the region of the satellite peak for the symmetrical structure. The inelastic processes contributing to the peaks a) and b) are represented in the inset.

N_w are the number of sites in the left and right barriers and the well, the associated widths are $L_i = N_i a$. For translational symmetry along the interface, we consider a single phonon mode per transversal (parallel to the interface) state, with frequency ω_0 and localized in the structure region. While conservation of transverse electron’s momentum might not be fully realistic [19], it constitutes a first approximation yielding results consistent with the main experimental features. The current components are obtained from (12) by integration over the transversal modes. The parameters in our calculations are chosen to simulate the case of a GaAs-AlGaAs structure. The effective mass m^* is 0.067 m_e , the LO phonon frequency $\hbar\omega_0 = 36$ meV, $a = 2.825$ Å, and the hopping parameter $V = 7.125$ eV. A typical e-ph interaction strength of $g \sim 0.1$ is obtained with $V_g \simeq 10$ meV. For a well of 56.5 Å, barrier heights of 300 meV and $\varepsilon_F = 10$ meV, the inclusion of $n \leq 3$ warrants good numerical convergence.

For wide left barriers (of about $25a \simeq 70$ Å or more), we found that the maximum value of P_{in} varies slowly with the width of the right barrier. Hence, consistently with our discussion of the 1-d model, there is no substantial gain in P_{in} by choosing an asymmetric structure. Consequently, a high phonon emission rate should be seek for thin barriers.

A thin left barrier of $L_L = 7a$ (19.7 Å), gives a tunneling probability $T_L(\varepsilon_F) = \Gamma_L / \Gamma \sim 0.03$. Fig. 2 shows the I-V curves for symmetric and asymmetric RTDs. In Fig. 3 we show $P_{\text{in}} - V$ for various right barrier widths L_R . The peaks are shifted to higher voltages as L_R is increased, because the resonant energies are lowered approximately by αeV . We can also see that the peak value of P_{in} as a function of the right barrier width exhibits a maximum.

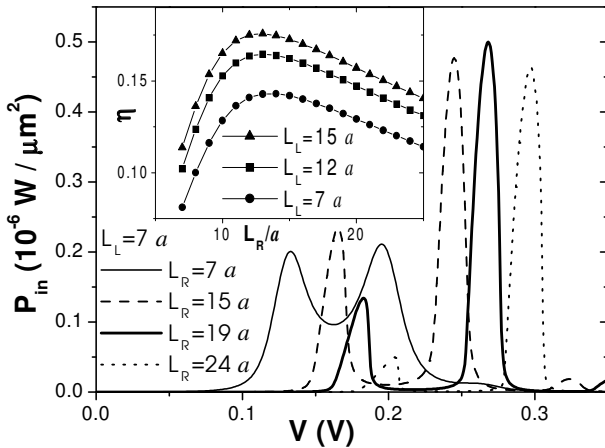


FIG. 3. Power emitted as LO phonons as a function of the applied voltage for $L_L = 7a$ (19.7 Å) and different values of L_R . The efficiency as a function of the right barrier width is shown in the inset.

The I-V curve for the optimal configuration is shown in Fig. 2 (heavy line). The inset of Fig. 3 shows the dependence of η , evaluated at the optimal voltage, on the right barrier width for various left barrier widths where $\Gamma_L < \hbar\omega_0$. In agreement with our theoretical analysis, η keeps the same magnitude for all the shown geometrical configurations. The main result of Fig. 3 is the confirmation that, for a given L_L satisfying $\Gamma_L < \hbar\omega_0$ and $g\Gamma_L + \Gamma_R > \varepsilon_F$, the phonon emission rate is enhanced by a factor 2.5 by choosing a wider right barrier as prescribed by Eq.(11). This may explain the unusually large satellite peaks of asymmetric structures [19].

An RTD optimized for phonon emission might have many applications. In fact, in AlGaAs-GaAs RTD these primary LO phonons have a short life-time [20] and decay into a pair of LO and transverse acoustic (TA) phonons. This phenomenon inspired the proposal [11] for the generation of a coherent TA-phonon beam in an RTD (called a SASER) [21]. That device *required* an energy difference between the first two electronic states in the well $E_1 - E_0 = \hbar\omega_0$ [11,21]. In contrast, the *present* proposal does not require such an accurate device geometry. Instead, operation in the phonon emission mode *only* requires the tuning of the many-body resonance with the external voltage. Geometry just improves its yield by imposing a generalized symmetry condition in the Fock-space. For a typical AlGaAs emitter barrier of 20 Å this would require a 54 Å collector's barrier. We expect that our results could stimulate the search for excited phonon modes (e.g. with Raman spectroscopy), in operational RTD's as a function of the applied voltage in the various configurations. While for simplicity we have restricted our analysis to a simple model of an RTD, a similar procedure can be applied to other problems and models involving electronic resonant tunneling in the presence of

an interaction with an elementary excitation.

We acknowledge financial support from CONICET, SeCyT-UNC, ANPCyT and Andes-Vitae-Antorchas. HMP and LEFFT are affiliated with CONICET.

* Corresponding author e-mail: horacio@famaf.unc.edu.ar

- [1] L. P. Kouwenhoven et al., in *Mesoscopic Electron Transport*, L. L. Sohn, L. P. Kouwenhoven and G. Schön, Eds. Kluwer 1997
- [2] C. Joachim, J. K. Gimzewski and A. Aviram. *Nature*, **408**, 541 (2000)
- [3] R. Landauer, *Phys. Lett.* **85A**, 91 (1981)
- [4] M. Büttiker, *Phys. Rev. Lett.* **57**, 1761 (1986)
- [5] V. J. Goldman, D. C. Tsui, and J. E. Cunningham, *Phys. Rev. B* **36**, 7635 (1987); M. L. Leadbeater et al., *Phys. Rev. B* **39**, 3438 (1989); G. S. Boebinger et al., *Phys. Rev. Lett.* **65**, 235 (1990).
- [6] B. C. Stipe, M. A. Rezaei, and W. Ho, *Phys. Rev. Lett.* **81**, 1263 (1998); H. Park et al., *Nature* **407**, 57 (2000).
- [7] N. S. Wingreen, K. W. Jacobsen, and J. W. Wilkins, *Phys. Rev. Lett.* **61**, 1396 (1988).
- [8] R. G. Lake, G. Klimeck, M. P. Anantram and S. Datta, *Phys. Rev. B* **48**, 15132 (1993).
- [9] S. Datta, *Phys. Rev. B* **40**, 5830 (1989).
- [10] J. L. D'Amato and H. M. Pastawski, *Phys. Rev. B* **41**, 7411 (1990); see also H. M. Pastawski and E. Medina, *Rev. Mex. Fis.*, **47S1,1** (2001) and cond-mat/0103219.
- [11] E. V. Anda, S. S. Makler, H. M. Pastawski, and R. G. Barrera, *Braz. J. Phys.* **24**, 330 (1994).
- [12] J. Bonča and S. A. Trugman, *Phys. Rev. Lett.* **75**, 2566 (1995); **79**, 4874 (1997).
- [13] P. Levstein, H. M. Pastawski, and J. L. D'Amato, *J. Phys. Condens. Matter* **2**, 1781 (1990).
- [14] J. L. D'Amato, H. M. Pastawski, and J. F. Weisz, *Phys. Rev. B* **39**, 3554 (1989).
- [15] U. Fano, *Phys. Rev.* **124**, 1866 (1961).
- [16] J. Göres et al., *Phys. Rev. B* **62**, 2188 (2000).
- [17] H. M. Pastawski, *Phys. Rev. B* **46**, 4053 (1992).
- [18] E. G. Emberly and G. Kirczenow, *Phys. Rev. B* **61**, 5740 (2000).
- [19] P. J. Turley, C. R. Wallis, S. W. Teitsworth, W. Li and P. K. Bhattacharya, *Phys. Rev. B* **47**, 12640 (1993).
- [20] F. Vallée, *Phys. Rev. B* **49**, 2460 (1994).
- [21] S. S. Makler, M. I. Vasilevskiy, E. V. Anda, D.E. Tuyarot, J. Weberszpil, and H. M. Pastawski, *J. Phys. Condens. Matter* **10**, 5905 (1998); I. Camps and S. S. Makler, *Solid State Commun.* **116**, 191 (2000).